A parafusin-related *Toxoplasma* protein in Ca^{2+}-regulated secretory organelles

Steen H. Matthiesen[a], Shailesh M. Shenoy[a], Kami Kim[b], Robert H. Singer[a], Birgit H. Satir[1)a]

[a] Department of Anatomy and Structural Biology, Albert Einstein College of Medicine, Bronx, NY/USA
[b] Department of Medicine and Department of Microbiology and Immunology, Albert Einstein College of Medicine, Bronx, NY/USA

Received June 12, 2001
Received in revised version September 10, 2001
Accepted September 13, 2001

Exocytosis – PGM superfamily – PRP1 – Toxoplasma gondii – 3-D deconvolution

We cloned a gene, *PRP1*, of *Toxoplasma gondii* encoding a 637-amino-acids protein having a calculated mass of 70 kDa. The sequence showed high homology to parafusin, a protein that in *Paramecium tetraurelia* participates in Ca^{2+}-regulated exocytosis and is a paralog of phosphoglucomutase. We show that *Toxoplasma gondii* homogenate and an expressed recombinant PRP1 fusion protein cross-react with a specific peptide-derived antibody to parafusin in Western blots. Antibodies to the recombinant PRP1 showed cross-reaction with parafusin and recognized PRP1, as bands at M_r 63×10^3 and 68×10^3, respectively. PRP1 is labeled when *Toxoplasma gondii* cells are incubated with inorganic ^{32}P and appears as the major band on autoradiograms of SDS-PAGE gels. The localization of PRP1 was examined in secretory organelles of *Toxoplasma gondii* by deconvolution light microscopy followed by three dimensional reconstruction using pairwise combinations of specific antibodies. PRP1 localized to the apical third of the cell. It co-localized with micronemes, the only secretory organelle the secretion of which is Ca^{2+} dependent. Quantification of the co-localized stain suggests that only mature micronemes ready for exocytosis have PRP1. These findings suggest that PRP1, parafusin and other members of the phosphoglucomutase superfamily have a conserved role in Ca^{2+}-regulated exocytic processes.

Abbreviations. AECOM Albert Einstein College of Medicine. – EPR Exhaustive photon reassignment. – EST Expressed sequence tags. – GST Glutathione S-transferase. – HFF Human foreskin fibroblasts. – PBS Physiologically buffered saline. – PFUS Parafusin. – PGM Phosphoglucomutase. – *PRP1* PFUS-related protein gene. – PRP1 Gene product of *PRP1*. – RBMPGM Rabbit muscle PGM. – rPRP1 GST-PRP1 fusion protein. – *T. gondii Toxoplasma gondii.*

Introduction

The apicomplexan protozoan *Toxoplasma gondii* (*T. gondii*) is an obligate intracellular parasite that enters mammalian cells by active invasion. Exocytosis of apical secretory organelles is essential for invasion of host cells (Dubremetz et al., 1998). *Plasmodium*, the malaria agent, is the most lethal of the Apicomplexa, but *T. gondii* is the most widespread, both in geographical and host range distribution. *T. gondii* is associated with severe birth defects and with opportunistic infections in AIDS patients. *T. gondii* contains three types of secretory organelles: micronemes, rhoptries and dense granules (Ngo et al., 2000). Secretion from these organelles during invasion has been examined (Carruthers and Sibley, 1997, 1999). The complete invasion process takes place within 25 – 40 s (Morisaki et al., 1995). Ca^{2+}-dependent release of micronemes takes place immediately after binding of the parasite to host cells (Carruthers and Sibley, 1999). As the host membrane invaginates to create the parasitophorous vacuole, rhoptry contents are released. Rhoptry discharge completes the invasion. Then dense granule contents are released into the formed parasitophorous vacuole. Although the exact molecular triggers for secretion in *T. gondii* have not been determined, the timing of secretion of each of the organelles in the process of invasion implies the presence of specific regulatory signals.

Apicomplexan protozoan and ciliates are phylogenetically related (Sogin and Silberman, 1998) and similar morphological functional features are present. In *Paramecium*, the structure of the membrane fusion site as seen with freeze fracture consists of an outer ring of particles, surrounding a central group of particles – called the fusion rosette (Satir et al., 1972, 1973; Beisson et al., 1976). At the anterior end of *T. gondii* a similar fusion rosette has been observed in the outer membrane of the

[1)] Dr. Birgit H. Satir, Department of Anatomy and Structural Biology, Albert Einstein College of Medicine, 1300 Morris Park, Bronx, NY 10461/USA, e-mail: bsatir@aecom.yu.edu, Fax: +1 718 430 8996.
Movies available online: http://singerlab.aecom.yu.edu/bhsatir/toxoplasma/

0171-9335/01/80/12-775 $15.00/0

pellicle near the terminal location of the rhoptries and micronemes beneath the plasma membrane (Porchet and Torpier, 1977). Both protozoa have a continuous membrane system, alveolar sacs, which underlie the plasma membrane. In *Paramecium* these sacs are Ca^{2+} storage compartments, analogous to the sarcoplasmic reticulum in muscle cells (Stelly et al., 1991, 1995). This suggests that the secretory processes in *T. gondii* and *Paramecium* have similar features.

Several genes for members of the phosphoglucomutase (PGM) superfamily in *Paramecium* have previously been cloned (Subramanian et al., 1994; Hauser et al., 1997). The gene product(s) that is related to Ca^{2+}-regulated exocytosis is known as parafusin (PFUS) (Gilligan and Satir, 1982) or PP63 (Hohne-Zell et al., 1992). PFUS is involved in regulated secretion in *Paramecium* (Gilligan and Satir, 1982; Zieseniss and Plattner, 1985; Satir et al., 1990; Subramanian and Satir, 1992; Subramanian et al., 1994). PFUS is associated with the cell membrane at the fusion rosette site and coats the secretory vesicles (Satir, 1989; Zhao and Satir, 1998).

In this study we report cloning, sequencing and expression of a gene expressing a *T. gondii* PFUS/PGM ortholog. The protein is referred to as PRP1 for parafusin-related protein and is recognized by a PFUS-specific antibody in Western blots. This protein incorporates $^{32}P_i$, and is localized to the cell apex. Using deconvolution microscopy, 3-D rotational reconstruction and quantification, PRP1 localizes with micronemes, the Ca^{2+}-dependent secretory organelles. This suggests that PRP1 and other PFUS orthologs have a conserved role in Ca^{2+}-dependent exocytosis.

Materials and methods

Cell lines, cell culture and harvesting

T. gondii, strain RH, was grown in human foreskin fibroblasts (HFF) in Dulbeccos's modified Eagle medium (Life Technologies, Grand Island, NY/USA) supplemented with 10% fetal bovine serum (Life Technologies) and 2 mM glutamine. Cultures were maintained at 37 °C in 5% CO_2. The tachyzoites (invasive stage of *T. gondii*) were collected by centrifugation (400*g*, 10 min). After washing, either in Hanks' balanced salt solution (Life Technologies) or physiologically buffered saline (PBS), cells were passed through 20 to 25-gauge needles, then separated from host cell material by passage through a 3.0 µm-pore Nucleopore filter. The tachyzoites were further washed 2 times in PBS before use.

Nucleic acid preparation

Genomic DNA was isolated from harvested, lysed tachyzoites using the Wizard genomic DNA purification system (Promega, Madison, WI/USA). Total RNA was isolated, either from lysed parasites or dividing parasites isolated from HFF, with TRIzol reagent (Life Technologies) following the manufacturer's directions.

Identification of PRP clones

Search of expressed sequence tags (EST) in the *T. gondii* database (http://www.cbil.upenn.edu/ParaDBs/Toxoplasma/index.html) revealed 4 cDNA clones with homology to PFUS/PGM (N60421, N61642, N60299, W06169). From these, three oligonucleotide primers were made (5′-GTCCGTATGCCGAGAAG-3′; 5′-CCTGTGCCGAAAG-ACTCT-3′; 5′-CGTAATGACAGTTGGCGT-3′). RNA from tachyzoites was used for RT-PCR. Single-strand cDNA was synthesized from total RNA using Superscript II (Life Technologies) according to the manufacturer's instructions. Single bands of the predicted sizes (1.1 kb and 0.55 kb) were obtained. These were gel purified, subcloned into pGEM-T (Promega), and 2 independent subclones from each PCR procedure were sequenced. All 4 clones were identical to each other in overlapping areas and to the EST sequences. The PCR clone containing the longest coding area was re-amplified by PCR in the presence of dig-11-dUTP (Boehringer Mannheim, Germany) and used to screen a *T. gondii* (strain RH) cDNA library. Hybridization analysis was carried out at 68 °C overnight using an optimized digoxigenin hybridization protocol (Engler-Blum et al., 1993). Positive clones were identified by BCIP/NBT (Bio-Rad, Hercules, CA/USA) detection of alkaline phosphatase-conjugated anti-digoxigenin antibody (Boehringer). Fourteen positive clones were identified. Two of these (C20 and C30) contained the entire open reading frame and were sequenced on both strands. DNA sequencing was performed using an Applied Biosystems automated DNA sequencer (DNA Sequence Facility, AECOM, NY/USA). The nucleotide sequence and deduced protein sequence were submitted to GenBank (AF295534).

DNA sequence and protein analysis

Analysis of the data was carried out using DNASTAR (1998 ed., Madison, WI/USA) or GCG (Version 9, Genetics Computer Group, Madison, WI/USA). The alignment was performed using an alignment algorithm (Needleman and Wunsch, 1970) modified to penalize gap insertions and deletions within regions of defined secondary structure (Lesk et al., 1986). Higher weights in alignment were given to areas important for the PGM activity, such as active-site loop and the Mg^{2+}-binding site. Functional significance of the amino acid replacement for the alignment was calculated using POLINA (Levin and Satir, 1998).

Southern and Northern blot analysis

PCR-amplified digoxigenin probes (using C20 as a template) were used for blotting analysis. The chemiluminescent alkaline phosphatase substrate CSPD® (Boehringer) was utilised for detection of hybridizing bands following the DIG System User's Guide (Boehringer). For Southern blots 6 µg genomic DNA were digested with the restriction enzymes: Bam H I, Bgl II, Cla I, EcoR I, Hind III, Kpn I, Nco I, Pst I, Sac I, Sac II, Sin I, Sma I, Xho I, Xba I and separated on a 0.8% agarose gel. The genomic Southern blotting was performed at high stringency (68 °C) as described for library screening after alkaline transfer of DNA to Hybond-N^+ membranes (Amersham Pharmacia Biotech, Piscataway, NY/USA). The following 5 PCR probes from the PRP1 cDNA were used for the hybridization: 373 – 615, 373 – 1911, 760 – 1911, 1128 – 1259 and 1540 – 1911 bp. For Northern blotting, 10 µg total RNA was separated on a 1.2% agarose/formaldehyde gel and transferred by downward capillary action to positively charged nylon membranes (Boehringer) and fixed by UV irradiation. The membranes were blocked in Dig Easy Hybe (Boehringer) and hybridization was carried out overnight with a DNA probe (373 – 1911 or 760 – 1911, see above) at 55 °C.

Expression of PRP1 in *E. coli*

A 1.6-kb Nco I fragment beginning at the deduced start codon and encompassing 86% of the coding region was cut out from C20, gel purified with the QIAquick gel extraction kit (Qiagen, Valencia, CA/USA), and cloned into the Nco I site of pGEX-kg (Guan and Dixon, 1991). To produce the glutathione S-transferase (GST)-PRP1 fusion protein, an overnight culture of DH10B (Gibco, BRL) carrying pGEX-kg:PRP1 was inoculated into LB medium containing 0.1 mg/ml ampicillin and grown at 30 °C to a density of 1.0 OD_{600}. 0.1 mM isopropyl-β-D-thiogalactopyranoside (IPTG) was added for 3 h at 30 °C. Bacteria were harvested, resuspended in PBS and lysed by sonication. After the insoluble fraction was removed by centrifugation (13000*g* for 30 min at 4 °C), a 50% v/v slurry of glutathione Sepharose® 4B beads (Amersham Pharmacia Biotech) in PBS was added and incubated at room temperature for 30 min. Beads were recovered by centrifugation and washed 3 times with PBS. The protein was eluted by 4 successive incubations for 20 min each at room temperature with 50 mM Tris-HCl, pH 8.0, containing 10 mM reduced glutathione. The GST-PRP1 was dialyzed against protein storage buffer (10 mM PIPES, 1 mM DTT, 0.1 mM EDTA, 0.02% NaN_3, 25% glycerol, pH 7.0) at 4 °C overnight.

Antibodies and peptides

I-2 is an affinity-purified rabbit anti-peptide antibody (0.51 mg/ml) prepared against a peptide sequence (I-2; DYEFEKHINLDQ) present in the *Paramecium* PFUS protein (Subramanian et al., 1994; Zhao and Satir, 1998). The homologue *T. gondii* PRP1 I-2 peptide, KFSIDKLGVQVNIDG, was synthesized and verified by mass spectrometry and HPLC (Laboratory for Macromolecular Analysis, AECOM/USA). The following *T. gondii* organelle-specific content antibodies were used: *1*) 92.10B and T62H11 against GRA1 and GRA3 proteins in dense granules; *2*) T34A11 and T42F3 against MIC2 and MIC3 proteins in micronemes; *3*) TG49 and T34A7 against ROP1 and ROP2,3,4 proteins in rhoptries; respectively. These antibodies are all monoclonal mouse antibodies except for TG49, which is a polyclonal rabbit antibody. The rPRP1-specific antibody was generated against purified recombinant GST-PRP1 (rPRP1) in female Balb-c mice from Jackson Laboratory (Bar Harbor, ME/USA).

Immunoblotting

SDS-PAGE was performed with lysates from isolated tachyzoites, *Paramecium* homogenates and purified recombinant PRP1 on 10% polyacrylamide gels (Laemmli, 1970). The proteins were transferred to nitrocellulose membranes (Schleicher and Schuell, Keene, NH/USA) using semi-dry electroblotting. After blocking in Tris-buffered saline/5% nonfat milk for 1 h, blots were incubated with primary antibody (I-2 antibody 1:500 and rPRP1 antibody 1:600) for 1.5 h at room temperature and washed. The blots were incubated with horseradish peroxidase (HRP)-conjugated anti-rabbit or -mouse IgG antibody (Boehringer) for 30 min and washed again. Labeled proteins were visualized by chemiluminescence detection of HRP activity (NEN™Life Science Products, Boston, MA/USA). In the competition experiment, 0.2 μM I-2 PFUS peptide was added to the primary I-2 antibody and then immediately incubated with the blot.

Immunoprecipitation

Tachyzoites were harvested (see above) using MOPS buffer (20 mM MOPS, 37 mM NaCl, 2.7 mM KCl, pH 7.4), and 1.5×10^8 cells were incubated with 15 μCi $^{32}P_i$ (NEN™Life Science Products) at 37 °C for 30 min. Then cells were centrifuged (1000*g* for 2 min), resuspended in 1 ml lysis buffer (50 mM Tris-HCl, pH 7.5, 150 mM NaCl, 1% Triton X-100, 5 mM EDTA, 2 μM leupeptin, 1.5 μM antipain, 0.5 mM PMSF, 0.012 TIU/ml aprotinin, 5 mM Na_3VO_4) and let stand for 20 min on ice. The lysate was centrifuged at 16000*g* for 5 min at 4 °C. Eight μl of the GST-PRP1 antibody was added and incubated at 24 °C for 1 h. Then 50 μl protein G beads (Sigma) (1:1 with lysis buffer) was added and held for 30 min at 4 °C. The beads were centrifuged and washed in lysis buffer and boiled for 5 min in 20 μl 2× SDS sample buffer. Subsequently, the sample was subjected to SDS-PAGE and autoradiography.

Immunofluorescence

The harvested tachyzoites (see above) were fixed in 3% paraformaldehyde in PBS for 20 to 30 min and permeabilized for 5 min in PBS, 0.1% Triton X-100. The cells were blocked in washing buffer (PBS, 3% albumin (bovine), 0.03% Tween20). The preparations were incubated with primary antibodies, I-2 (1:800), ROP2 (1:500), ROP2,3,4 (1:1000), MIC3 (1:1000) and GRA1 (1:100) for 15 min, washed, incubated with secondary FITC-labeled anti-mouse IgG (1:200) or CY3-labeled anti-rabbit IgG (1:1600) (Jackson ImmunoResearch Laboratories, West Grove, PA/USA) for 15 min and washed again. Then 3 ng/ml DAPI (Sigma) was added for 30 s, if the nucleus was to be stained, and the specimens were washed. TetraSpeck microphores (100 nm) fluorescing in blue/green/orange/deep red (Molecular Probes, Eugene, OR/USA) were included in the mounting medium (PBS, 70% glycerol, 2% N-propyl-gallate) and used as a fiduciary marker to align the optical sections. In the competition experiments, 0.1 μM I-2 PFUS peptide or 100 μM to 0.1 nM I-2 PRP1 peptide was added to the primary I-2 antibody and immediately incubated with the preparations.

Fluorescence microscopy, digital image acquisition, deconvolution, three-dimensional reconstruction and image analysis

Standard fluorescence imaging was performed using a BX60 microscope (Olympus, Melville, NY/USA) with a PlanApo 60×, 1.4 NA objective (Olympus) and High Q filter sets (Chroma Technology, Brattleboro, VT/USA). Images were acquired using a FKI1001 digital CCD camera (PerkinElmer Life Sciences, Boston, MA/USA) using Esprit software (PerkinElmer Life Sciences). Deconvolution imaging was performed using a Provis AX70 microscope (Olympus) with a PlanApo 60×, 1.4 NA objective (Olympus) and High-Q filter sets (Chroma Technology). Images were acquired using a 15-bit, cooled (−40 °C), digital CCD camera (model CH250, Roper Scientific, San Diego, Ca/USA) using CellScan software (Scanalytics, Fairfax, VA/USA). The objective was mounted in a piezoelectric translator (model P-721.10, Physik Instrumente, Costa Mesa, CA/USA) that positioned the objective in the axial direction, along the optical path, in 100-nm increments. For each fluorescence channel used, 33 wide-field images were acquired serially, separated by 100 nm axially, thus forming an over-sampled image volume composed of volume elements (or voxels) with dimensions of 100 nm on each side. Each image volume was deconvolved using iterative deconvolution with an acquired point spread function (Exhaustive Photon Reassignment (EPR) software, Scanalytics). A point spread function (PSF) was acquired in each fluorescence channel exactly as the specimen were acquired except that a minimum of 65 wide-field images, each separated by 100 nm axially, were acquired for each PSF. The EPR deconvolution parameters were set to 400 iterations, a smoothing value of 5×10^{-6} and a convergence of 0.001. The deconvolved image volumes were rendered and rotated using Intervision software (Noran Instruments, Middleton, WI/USA) on an O2 workstation (SGI, Mountain View, CA/USA).

The co-localization analysis was performed on deconvolved image volumes using software written in the laboratory (Fay et al., 1997). In each field, the cell boundaries were circled, with the aid of Nomarski images. The image volume was then segmented into one sub-volume for each cell. The mean and standard deviation of the fluorescence intensity within each sub-volume were calculated for both of the fluorescence channels being examined. A threshold was applied to each sub-volume equal to the mean plus five standard deviations of the intensities in that sub-volume. The software then determined the amount of co-localization by measuring the amount of overlap between the fluorescence in the two fluorescence channels being examined.

Results

Cloning of *PRP1* (parafusin-related protein 1)

The *T. gondii* EST database contains four cDNA clones with high homology to PFUS/PGM. These were used to select primers for RT-PCR synthesis of a 1.1-kb probe that was used to screen a *T. gondii* cDNA library. The nucleotide sequences were identical for the two full-length cDNA clones obtained. Alignment of the deduced amino acid sequence with PFUS and rabbit muscle PGM (RBMPGM) is shown in Fig. 1. The cloned gene was called *PRP1* (PFUS-related protein) and the gene product PRP1. PRP1 contains 637 amino acids and has a calculated molecular mass of 70 kDa. The N-terminal domain contains a putative N-myristoylation site (^{2}Gly). The amino acid sequence of PRP1 has about 50% identity (60% similarity) to both *Paramecium* PFUS and RBMPGM (Table I). Comparison of the I-2 regions reveals a block of four amino acids with 2 identical residues and 2 conservative substitutions (Fig. 1).

Results of genomic Southern blots of the tachyzoites under high stringency conditions were consistent with *PRP1* being a single-copy gene (Fig. 2A). Northern blot analysis of total RNA from both lysed and dividing tachyzoites showed one major

Fig. 1. Alignment of deduced amino acid sequences of selected members of the PGM superfamily: PRP1 – *Toxoplasma gondii* parafusin-related protein (accession number AF295534), PFUS – *Paramecium* parafusin (accession number L12471), RBMPGM – Rabbit muscle PGM (accession number P00949). Deletions and insertions present both in PFUS and PRP1, as compared to RBMPGM, are denoted by D# and I#, respectively; while deletions and insertions in PRP1 only are denoted by D#′ and I#′ and in *Paramecium* only by (D#) and (I#). Comparison of the I-2 region of *Paramecium* PFUS with *T. gondii* PRP1 is shown in *bold*. The *underlined* residues in PRP1 indicate the identical (*uppercase*) or highly conserved amino acids (*lowercase*). A potential myristoylation site at the second residue is indicated by an *asterisk*. Two regions important for PGM enzymatic activity are *shaded gray*: the active site, that has the serine *boxed black*, and the Mg^{2+}-binding site.

Tab. I. Comparison of PRP1 with two related proteins from a mammal and a ciliate

Similarity/identity	PRP1	RBMPGM	PFUS
PRP1	–	52.6	49.5
RBMPGM	61.0	–	54.7
PFUS	59.3	64.5	–

Amino acid identity is indicated above the diagonal and similarity below, both shown in %. Blosum 62 was used with a gap weight of 8 and a length weight of 2. See legend in Fig. 1 for accession numbers.

hybridizing band at 2.3 kb and a minor one at ≅2.7 kb (Fig. 2B). This result was obtained 3 times in blots using two different cDNA probes. No bands were observed with total RNA from uninfected cells (HFF).

Immunological characterization of PRP1

T. gondii PRP1 has an apparent M_r of 68×10^3 and specifically reacts with two antibodies: An antiserum against purified *T. gondii* GST-PRP1 fusion protein (rPRP1) and an antibody against *Paramecium* PFUS I-2 peptide. Western blot analysis with mouse antiserum to rPRP1 (Fig. 3A) showed a single band each for *Paramecium* PFUS (high-speed supernatant of *Paramecium* homogenate) at M_r 63×10^3, for tachyzoite lysates at 68×10^3 and for rPRP1 at M_r 85×10^3 (the expected size). A Western blot using I-2 antibody showed single positive bands at the same positions as those obtained with the rPRP1-specific antiserum (Fig. 3B). These signals were reduced when competed with the I-2 peptide, confirming the specificity (Fig. 3C). The I-2 antibody did not recognize either GST alone or GST-TPK3 (Qin et al., 1998), a non-relevant GST fusion protein (data not shown).

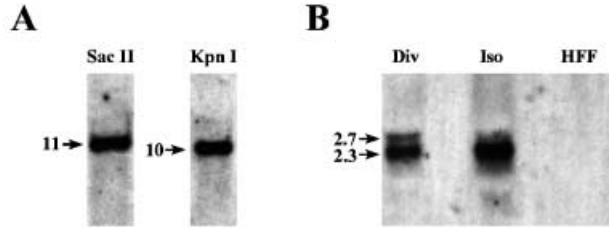

Fig. 2. Southern and Northern blots of *PRP1*. (**A**) The Southern blots indicating the presence of a single-copy gene. A probe ranging from 373–1911 bp of the coding sequence of the *PRP1* gene hybridized to single bands of Sac II- and Kpn I-digested genomic DNA as expected from the cDNA sequence. (**B**) The Northern blot shows that the gene is expressed. The *PRP1* gene is expressed in both dividing (Div.) and isolated *T. gondii* tachyzoites (Iso), but not in the parasite host cells (HFF). The same probe as in (**A**) was used for the hybridization. The arrows and numbers indicate the size of the DNA fragments in kbp or kilo bases, respectively.

Phosphorylation of PRP1

In vivo $^{32}P_i$ incorporation is one of the characteristics of *Paramecium* PFUS (Gilligan and Satir, 1982). Isolated tachyzoites were allowed to incorporate $^{32}P_i$ (20 min, 25 °C) and were prepared and run on SDS-PAGE, followed by autoradiography. The radiograms showed incorporation into a band at M_r 68×10^3 for the tachyzoite protein and M_r 63×10^3 for the PFUS control (Fig. 4). Immunoprecipitation with the rPRP1-specific antibody showed that the radioactively labeled protein at M_r 68×10^3 was PRP1 (Fig. 4).

Localization of PRP1 by immunofluorescence microscopy

PRP1 was localized in isolated tachyzoites by immunofluorescence using I-2 as primary antibody and fluorescence-labeled anti-rabbit IgG as secondary antibody (Fig. 5). The apical ends of the cells were strongly labeled (Fig. 5A). To ensure the specificity of the antibody, competition experiments were performed with both the PFUS I-2 peptide (Fig. 5C) and the PRP1 I-2 peptide (Fig. 5E). The apical staining was completely blocked by concentrations of peptide as low as 4 nM. Omission of primary antibody also resulted in no labeling (data not shown). PRP1 is thus present in the apical end of tachyzoites.

To determine whether PRP1 is associated with one or more of *T. gondii* secretory organelles double-labeling experiments were performed. Cells were labeled with I-2 antibody and with

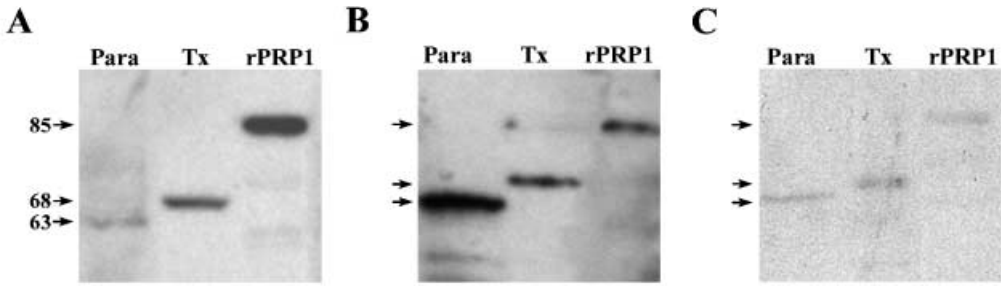

Fig. 3. Immunoblots show recognition of PRP1 by PRP1- and PFUS-specific antibodies. (**A**) Antiserum to PRP1 with high-speed supernatant fraction (100 000*g*) from *Paramecium* (Para), lysate of isolated *T. gondii* tachyzoites (Tx) and recombinant GST-PRP1 (rPRP1). (**B**) I-2 antibody with the same samples as shown in (**A**). (**C**) Same as (**B**) after being competed with 0.2 μM I-2 PFUS peptide under identical exposure time and conditions. The arrows and numbers ($\times 10^3$) indicate the M_r of the bands.

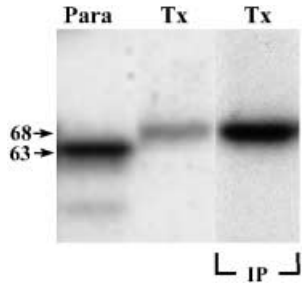

Fig. 4. In vivo phosphorylation shows the same characteristic labeling of PRP1 as observed for PFUS. Autoradiograms of in vivo incorporation of $^{32}P_i$. *Paramecium* (Para), isolated *T. gondii* tachyzoites (Tx) and immunoprecipitated PRP1 (IP) from tachyzoites with rPRP1-specific antibody.

antibodies to ROP2,3,4 (content of rhoptry), with antibodies to MIC3 (content of microneme) or with antibodies to GRA3 (content of dense granule). Results of the double labeling for ROP2,3,4 and MIC3 are shown in Figure 5G–M with the corresponding Nomarski images. The region of overlap (yellow) between PRP1 and antibodies to rhoptry and microneme content, respectively, is confined to the apical ends of the cells. No overlap of labeling is seen when cells were labeled with the I-2 antibody and the antibody to dense granule content (GRA3) (data not shown). Thus, PRP1 appears to be associated with the apically located rhoptries and micronemes. However, with these images it is not possible to differentiate the co-localization in rhoptries and micronemes. Therefore, deconvolution analysis and 3-D rotational reconstruction was used.

Localization of PRP1 by deconvolution analysis of immunofluorescent cells

Wide-field fluorescence microscopy and iterative image deconvolution with an acquired point spread function (EPR) was used to determine which secretory vesicles co-localized with PRP1. This methodology resolves the spatial separation of objects at a resolution of 100 nm (Carrington et al., 1995; Femino et al., 1998). Figure 6 shows representative results of this deconvolution analysis of image volumes of isolated tachyzoites double labeled with combinations of five different antibodies.

To show the efficiency of this technique, we labeled micronemes and rhoptries with appropriate antibodies resolving the separate organelles. Figure 6A shows an example of a tachyzoite labeled with antibodies to microneme contents (green, MIC3) and to rhoptry contents (red, ROP2). The labeling of these two types of secretory organelles is distinct and the weak overlap of content disappears when the rendered image volume

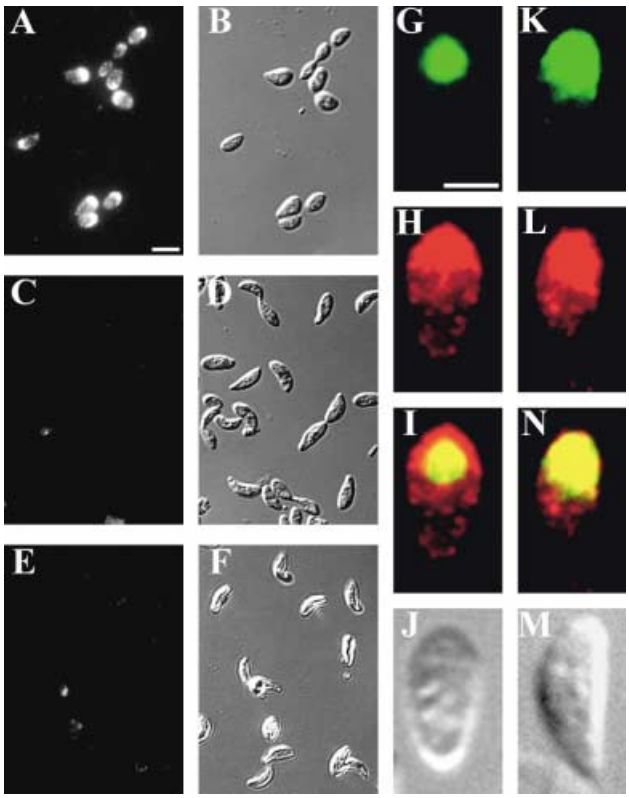

Fig. 5. Immunofluorescence labeling of *T. gondii* shows that PFUS I-2 antibody is specific for PRP1 and indicates that PRP1 is associated with secretory organelles. **A–F** Micrographs of isolated tachyzoites labeled with I-2 peptide antibody before and after competition with specific peptides (**A, C, E**). Immunofluorescent images (**A**) I-2 antibody labeling. (**C**) I-2 antibody competed with PFUS I-2 peptide (0.1 μM) from *Paramecium* and (**E**) competed with I-2 PRP1 peptide (4 nM) from *T. gondii*. (**B, D, F**), Nomarski images of (**A, C, E**). **G–N** Co-localization of organelle-specific antibodies and PRP1 to the apical end of tachyzoites (**I, N**). (**G**) ROP2,3,4 antibody (content of rhoptry). (**H**) I-2 antibody (PRP1). (**I**) Overlap indicated in yellow in the superimposed image. (**J**) Nomarski image of the cell shown in (**G–I**). (**K**) MIC3 antibody (content of microneme). (**L**) I-2 antibody (PRP1). (**N**) Overlap indicated in yellow in the superimposed image. (M) Nomarski image of the cell shown in (**K–N**). Scale bars in (**A–F**) represent 5 μm and 2 μm in (**G–M**).

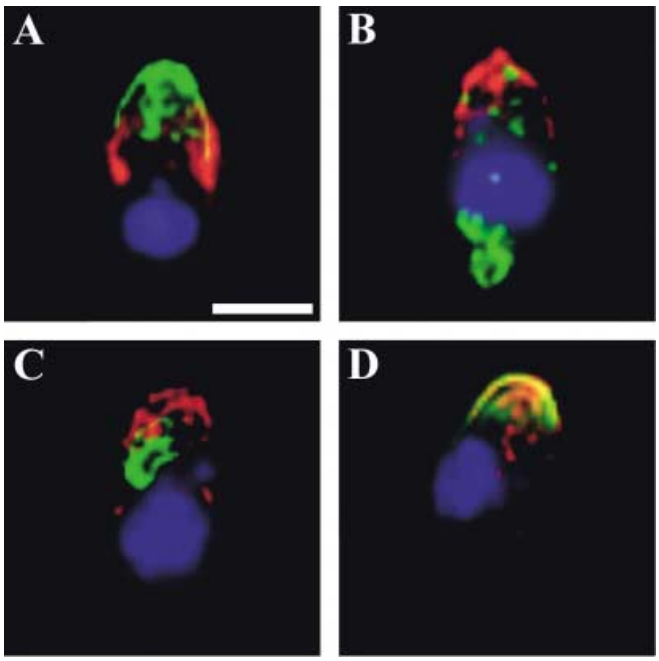

Fig. 6. PRP1 co-localizes principally with micronemes. 3-D reconstruction of deconvolved fluorescence light microscope images of isolated, double-labeled tachyzoites. Overlap shown in yellow. The methodology separates two closely positioned organelles. (**A**) Micronemes (MIC3 antibody) *green* and rhoptries (ROP2 antibody) *red* demonstrate organelle separation. (**B**) Dense granules (GRA1 antibody) *green* and PRP1 (I-2 antibody) *red*. (**C**) Rhoptries (ROP2/3/4 antibody) *green* and PRP1 (I-2 antibody) *red*. (**D**) Micronemes (MIC3 antibody) *green* and PRP1 (I-2 antibody) *red* show co-localization. Each image consists of multiple superimposed translucent planes, (**A**) 24 planes, (**B**) 25 planes, (**C**) 20 planes and (**D**) 21 planes, with a z-value of 100 nm. The nucleus is marked in blue (DAPI) and not deconvolved. The scale bar represents 2 μm.

is rotated (see upper panel Fig. 7 and online movie: http://singerlab.aecom.yu.edu/bhsatir/toxoplasma/). Most of the micronemes form an extended apical cap quite distinct from the thinner basal end of the rhoptries and are not confined to the center of the tachyzoite. ROP2 antibodies are not localized in the thin extensions of the rhoptries that run from the body towards the fusion rosette in the center of the cell apex.

In cells labeled with antibodies against the content of dense granules (green, GRA1) or rhoptries (green, ROP2,3,4) and against PRP1 (red) (Fig. 6B and C), no overlap was observed (see movies online). In contrast, labeling of microneme content (green, MIC3) and PRP1 (red) demonstrates co-localization as a bright yellow cap of fluorescence at the apical end of the cell (Fig. 6D) which persisted when the image volume was rotated (Fig. 7, lower panel). This co-localization can be visualized in a movie showing the rotation of the rendered image volume (see movie online). The percentage of co-localization was quantified in three dimensions (Fig. 8). Double labeling for PRP1 together with other organelle content-specific antibodies (MIC2, GRA3 and ROP1) gave the same labeling pattern as observed with antibodies against MIC3, GRA1 and ROP2,3,4 (data not shown).

Quantitation of such images (Fig. 8, 24% of the voxels measured in 26 cells) shows that microneme content co-localized with PRP1. In contrast, less than 3% of voxels associate with dense granule or rhoptry content co-localized with PRP1, with significant p values ($< 1.6 \times 10^{-10}$, and 2.0×10^{-11}, respectively). The voxels associated with both micronemes and PRP1 are spread in a thin rim at the cell apex, when the view is longitudinal, and a cap when the view is more frontal, which corresponds to microneme distribution as observed at the cell apex and not to the central bundle of the ends of rhoptries. However, sometimes a central core of PRP1 label not associated with micronemes is seen (see movie online or Fig. 7, lower panel). We conclude that PRP1 localizes principally to a rim of apical micronemes in *T. gondii* tachyzoites.

Discussion

PRP1, a member of the PGM superfamily was cloned and sequenced in *T. gondii*. *PRP1*, which is a homologue of PFUS, appears to be a single-copy gene as evidenced by hybridization data shown in Figure 2A and hybridization patterns of different probes used in Southern blot analysis with genomic DNA digested with combinations of different restriction enzymes

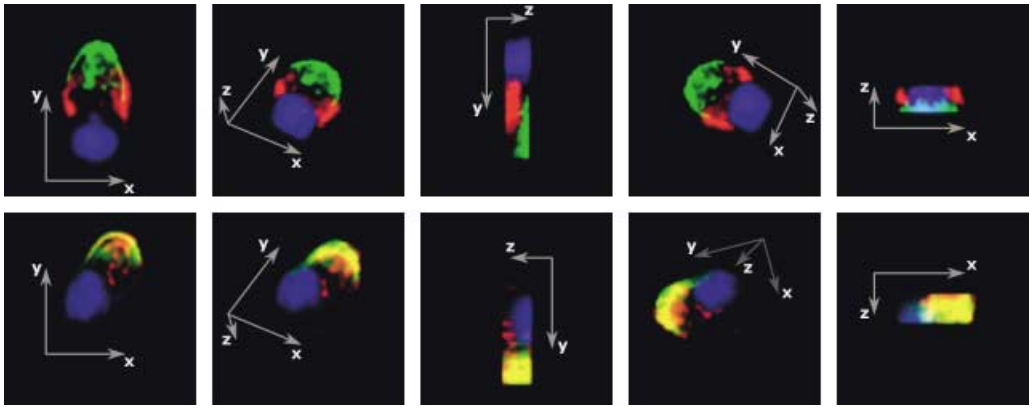

Fig. 7. 3-D reconstruction of deconvolved images. Image volumes of cells A and D of Fig. 6 shown from five perspectives. *Left panels*: conventional right-handed axis (longitudinal view). *Upper panel*: Image volumes of the cell shown in panel A of Fig. 6. At no point are there voxel overlaps between micronemes (MIC3 antibody, *green* channel) and rhoptries (ROP2 antibody, *red* channel), demonstrating clear separation of the two types of fluorescently labeled organelles. *Lower panel*: The thin yellow cap that fills most of the apex of the cell represents voxel overlap between PRP1 (I-2 antibody, *red* channel) and micronemes (MIC3 antibody, *green* channel).

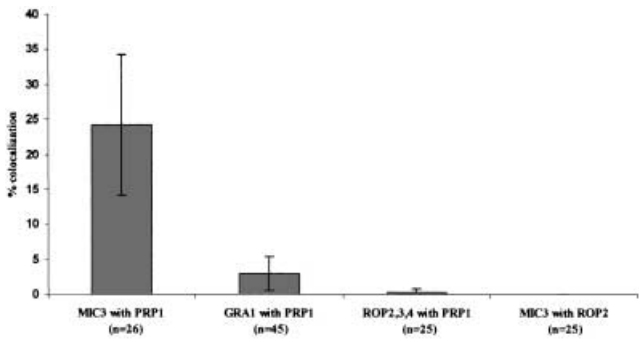

Fig. 8. The quantitative analysis of co-localization obtained from three separate experiments confirms the qualitative observations, made in Figs. 6 and 7, that PRP1 is principally localized to the micronemes. Some minor co-localization is indicated between PRP1 and dense granules. Separation of micronemes and rhoptries is demonstrated by the lack of co-localization between antibodies to their respective contents. The standard deviations are indicated by the bars.

(not shown; see Materials and methods). These patterns make it unlikely that *PRP1* has dispersed paralogs or paralogs arrayed in tandem. Modeling results indicate that PRP1 has maintained the same basic structure as RBMPGM. The region of the catalytic site (^{116}Ser) is conserved in the primary structure as found in other members of this superfamily (Levin et al., 1999). All insertions (I) and deletions (D), compared with RBMPGM, are located in surface loops of the protein PRP1 as observed for PFUS (Levin et al., 1999). A special feature of PRP1 is the presence of a putative N-myristoylation site at the amino terminus (^{2}Gly) since this suggests a possible means of membrane association.

PRP1 and PFUS have 53 and 55% sequence identity to rabbit muscle PGM at the amino acid level, respectively, and 50% to each other. PGM is a cytosolic glycolytic enzyme that interconverts glucose-1-phosphate to glucose-6-phosphate by transferring the phosphate residue at C_1 from glucose-1,6-bisphosphate onto glucose-1-phosphate resulting in glucose-6-phosphate and glucose-1,6-bisphosphate. Different paralogs or isoforms of PGM exist with a variety of functions within a cell. Therefore, in addition to the classical function of PGM in glucose metabolism, some members of the PGM superfamily appear to function in Ca^{2+}-mediated signaling events in a variety of eukaryotic cells and tissues (Lee et al., 1992; Kim et al., 1992; Subramanian and Satir, 1992; Subramanian et al., 1994; Zhao and Satir, 1998; Kissmehl et al., 1998; Fu et al., 2000).

In immunofluorescence microscopy, the binding of the PFUS-specific rabbit I-2 antibody was competed with both the I-2 peptide used to generate the antibody and the homologous peptide from *T. gondii*. The results confirm a high specificity of the I-2 peptide antibody to PRP1. Immunoblot analyses also indicate that the I-2 antibody identifies the *T. gondii* PRP1.

In *T. gondii*, deconvolution analyses and computer volume reconstructions were undertaken to clarify the localization of PRP1, since both micronemes (100 nm in length) and the larger and longer rhoptries (3–4 μm) reside in the apical end of the cell. Specific association of PRP1 with micronemes could be established after 3-D rotational views of differently double-labeled specimens were generated, establishing that overlap in single optical sections was not artifactual.

We hypothesize that PRP1 probably is part of a peripheral "coat" of proteins that surrounds micronemes similar to what has been observed with PFUS in *Paramecium*. It is interesting that quantitatively 24% of voxels show co-localization of MIC 3, the marker of microneme content, with PRP1. Since this number is in agreement with the fraction of microneme proteins released upon invasion ($24 \pm 8\%$) (Carruthers et al., 1999), PRP1 may associate with the subpopulation of micronemes competent for secretion.

Ciliates and Apicomplexan protozoa are relatively closely related (Sogin and Silberman, 1998). Therefore, it might be expected that their mechanisms of regulated secretion have features in common. In addition to the association of PRP1/PFUS with Ca^{2+}-regulated secretory vesicles, a fusion rosette similar to that observed in *Paramecium* is present in *T. gondii* (Satir et al., 1972; Beisson et al., 1976; Porchet and Torpier, 1977). Other characteristics of PRP1 in common with those of *Paramecium* PFUS have been defined by this study, e.g. a similar I-2 region of the proteins and incorporation of $^{32}P_i$ into PRP1 in living cells, suggesting common biochemical modifications. We conclude that PRP1 is the PFUS ortholog of *T. gondii*. Conservation of PRP1 in Ca^{2+}-regulated exocytosis would not be surprising because many components for secretion seem to be evolutionarily conserved in *T. gondii* (Chaturvedi et al., 1999; Hoppe et al., 2000).

A gene knockout of an ortholog of PFUS/PGM has been done in the protozoan *Tetrahymena* (Chilcoat and Turkewitz, 1997). It showed no phenotypic changes with regard to growth and exocytosis. However, the kinetics and amount of secretion were not examined. Gene knockout experiments do not always produce a clear new phenotype (Geppert et al., 1994, 1997; Liu et al., 1993; Cook et al., 1997; Madhani et al., 1997). The reason why no phenotypic change was observed in the *Tetrahymena* knockout could be due to substitute pathways or redundancy.

Recently, it was shown that the knockout of the major isoform of PGM (pgmΔ2) in *Saccharomyces cerevisiae* led to a 5-fold increase in the Ca^{2+} uptake rate resulting in a 9-fold increase in total cellular Ca^{2+} (Fu et al., 2000). The pgmΔ2 did not reduce the amount of Ca^{2+} present in the exchangeable pool, endoplasmic reticulum and Golgi, indicating that the depletion of the Ca^{2+} stores was not the source of the increased Ca^{2+} uptake rate. This suggests that some members of the PGM superfamily may play a role in Ca^{2+} influx and perhaps PRP1 functions in this way in Ca^{2+}-regulated exocytosis. Cellular Ca^{2+} levels have not been described in *Tetrahymena* knockout.

Ca^{2+}-dependent exocytosis of micronemes is the first step in the invasion process by *T. gondii* and other Apicomplexan parasites. PRP1 is principally associated with micronemes and not with rhoptries or dense granules, the release of which is thought to be Ca^{2+} independent. This observation strengthens the hypothesis that orthologs of PFUS have a conserved role in Ca^{2+}-dependent exocytosis. Discovering the role of PRP1 in this critical step may result in a better understanding of PGM superfamily members and provide new tools for blocking cell invasion by Apicomplexan parasites.

Acknowledgements. We thank Drs. P. Satir and M. Rapport for critical reading of the manuscript, and J. Tang and M. Reichman for technical assistance. The cDNA library was a gift of J. Ajioka, University of Cambridge, UK. 92.10B was provided by L. Weiss (AECOM, NY/USA), ROP2 by C. J. Beckers (University of Alabama, AL/USA), T34A11, T42F3 and T34A7 by J.-F. Dubremetz (INSERM, France), T62H11 and T34A7 by K. Joiner (Yale University School of Medicine, CT/USA) and TG49 by J. Schwartzman (Dartmouth Medical Center,

NH/USA). This work was supported by NSF grant MCB723532 and March of Dimes 6-FY00 – 144 (B. H. Satir), Burroughs Welcome New Investigator in Mol. Parasitology Award, AI01535, AI41058 (K. Kim) and "Thanks to Scandinavia" (S. H. Matthiesen).

References

Beisson, J., Lefort-Tran, M., Pouphile, M., Rossignol, M., Satir, B. (1976): Genetic analysis of membrane differentiation in *Paramecium*. Freeze-fracture study of the trichocyst cycle in wild-type and mutant strains. J. Cell Biol. **69**, 126 – 143.

Carrington, W. A., Lynch, R. M., Moore, E. D., Isenberg, G., Fogarty, K. E., Fay, F. S. (1995): Superresolution three-dimensional images of fluorescence in cells with minimal light exposure. Science **268**, 1483 – 1487.

Carruthers, V. B., Giddings, O. K., Sibley, L. D. (1999): Secretion of micronemal proteins is associated with *Toxoplasma* invasion of host cells. Cell. Microbiol. **1**, 225 – 235.

Carruthers, V. B., Sibley, L. D. (1997): Sequential protein secretion from three distinct organelles of *Toxoplasma gondii* accompanies invasion of human fibroblasts. Eur. J. Cell Biol. **73**, 114 – 123.

Carruthers, V. B., Sibley, L. D. (1999): Mobilization of intracellular calcium stimulates microneme discharge in *Toxoplasma gondii*. Mol. Microbiol. **31**, 421 – 428.

Chaturvedi, S., Qi, H., Coleman, D., Rodriguez, A., Hanson, P. I., Striepen, B., Roos, D. S., Joiner, K. A. (1999): Constitutive calcium-independent release of *Toxoplasma gondii* dense granules occurs through the NSF/SNAP/SNARE/Rab machinery. J. Biol. Chem. **274**, 2424 – 2431.

Chilcoat, N. D., Turkewitz, A. P. (1997): In vivo analysis of the major exocytosis-sensitive phosphoprotein in *Tetrahymena*. J. Cell Biol. **139**, 1197 – 1207.

Cook, J. G., Bardwell, L., Thorner, J. (1997): Inhibitory and activating functions for MAPK Kss1 in the *S. cerevisiae* filamentous-growth signalling pathway. Nature **390**, 85 – 88.

Dubremetz, J. F., Garcia-Reguet, N., Conseil, V., Fourmaux, M. N. (1998): Apical organelles and host-cell invasion by Apicomplexa. Int. J. Parasitol. **28**, 1007 – 1013.

Engler-Blum, G., Meier, M., Frank, J., Muller, G. (1993): Reduction of background problems in nonradioactive Northern and Southern blot analysis enables higher sensitivity than ^{32}P-based hybridization. Anal. Biochem. **210**, 235 – 244.

Fay, F. S., Taneja, K. L., Shenoy, S., Lifshitz, L., Singer, R. H. (1997): Quantitative digital analysis of diffuse and concentrated nuclear distributions of nascent transcripts, SC35 and poly(A). Exp. Cell Res. **231**, 27 – 37.

Femino, A. M., Fay, F. S., Fogarty, K., Singer, R. H. (1998): Visualization of single RNA transcripts in situ. Science **280**, 585 – 590.

Fu, L., Miseta, A., Hunton, D., Marchase, R. B., Bedwell, D. M. (2000): Loss of the major isoform of phosphoglucomutase results in altered calcium homeostasis in *Saccharomyces cerevisiae*. J. Biol. Chem. **275**, 5431 – 5440.

Geppert, M., Bolshakov, V. Y., Siegelbaum, S. A., Takei, K., De Camilli, P., Hammer, R. E., Südhof, T. C. (1994): The role of Rab3A in neurotransmitter release. Nature **369**, 493 – 497.

Geppert, M., Goda, Y., Stevens, C. F., Südhof, T. C. (1997): The small GTP-binding protein Rab3A regulates a late step in synaptic vesicle fusion. Nature **387**, 810 – 814.

Gilligan, D. M., Satir, B. H. (1982): Protein phosphorylation/dephosphorylation and stimulus-secretion coupling in wild type and mutant *Paramecium*. J. Biol. Chem. **257**, 13903 – 13906.

Guan, K. L., Dixon, J. E. (1991): Eukaryotic proteins expressed in *Escherichia coli*: an improved thrombin cleavage and purification procedure of fusion proteins with glutathione S-transferase. Anal. Biochem. **192**, 262 – 267.

Hauser, K., Kissmehl, R., Linder, J., Schultz, J. E., Lottspeich, F., Plattner, H. (1997): Identification of isoforms of the exocytosis-sensitive phosphoprotein PP63/parafusin in *Paramecium tetraurelia* and demonstration of phosphoglucomutase activity. Biochem. J. **323**, 289 – 296.

Hohne-Zell, B., Knoll, G., Riedel-Gras, U., Hofer, W., Plattner, H. (1992): A cortical phosphoprotein ('PP63') sensitive to exocytosis triggering in *Paramecium* cells. Immunolocalization and quenched-flow correlation of time course of dephosphorylation with membrane fusion. Biochem. J. **286**, 843 – 849.

Hoppe, H. C., Ngo, H. M., Yang, M., Joiner, K. A. (2000): Targeting to rhoptry organelles of *Toxoplasma gondii* involves evolutionarily conserved mechanisms. Nature Cell Biol. **2**, 449 – 456.

Kim, D. H., Lee, Y. S., Landry, A. B., 3rd. (1992): Regulation of Ca^{2+} release from sarcoplasmic reticulum in skeletal muscles. Mol. Cell. Biochem. **114**, 105 – 108.

Kissmehl, R., Hauser, K., Gossringer, M., Momayezi, M., Klauke, N., Plattner, H. (1998): Immunolocalization of the exocytosis-sensitive phosphoprotein, PP63/parafusin, in *Paramecium* cells using antibodies against recombinant protein. Histochem. Cell Biol. **110**, 1 – 8.

Laemmli, U. K. (1970): Cleavage of structural proteins during the assembly of the head of bacteriophage T4. Nature **227**, 680 – 685.

Lee, Y. S., Marks, A. R., Gureckas, N., Lacro, R., Nadal-Ginard, B., Kim, D. H. (1992): Purification, characterization, and molecular cloning of a 60-kDa phosphoprotein in rabbit skeletal sarcoplasmic reticulum which is an isoform of phosphoglucomutase. J. Biol. Chem. **267**, 21080 – 21088.

Lesk, A. M., Levitt, M., Chothia, C. (1986): Alignment of the amino acid sequences of distantly related proteins using variable gap penalties. Protein Eng. **1**, 77 – 78.

Levin, S., Almo, S. C., Satir, B. H. (1999): Functional diversity of the phosphoglucomutase superfamily: structural implications. Protein Eng. **12**, 737 – 746.

Levin, S., Satir, B. H. (1998): POLINA: detection and evaluation of single amino acid substitutions in protein superfamilies. Bioinformatics **14**, 374 – 375.

Liu, H., Styles, C. A., Fink, G. R. (1993): Elements of the yeast pheromone response pathway required for filamentous growth of diploids. Science **262**, 1741 – 1744.

Madhani, H. D., Styles, C. A., Fink, G. R. (1997): MAP kinases with distinct inhibitory functions impart signaling specificity during yeast differentiation. Cell **91**, 673 – 684.

Morisaki, J. H., Heuser, J. E., Sibley, L. D. (1995): Invasion of *Toxoplasma gondii* occurs by active penetration of the host cell. J. Cell Sci. **108**, 2457 – 2464.

Needleman, S. B., Wunsch, C. D. (1970): A general method applicable to the search for similarities in the amino acid sequence of two proteins. J. Mol. Biol. **48**, 443 – 453.

Ngo, H. M., Hoppe, H. C., Joiner, K. A. (2000): Differential sorting and post-secretory targeting of proteins in parasitic invasion. Trends Cell Biol. **10**, 67 – 72.

Porchet, E., Torpier, G. (1977): [Freeze fracture study of *Toxoplasma* and *Sarcocystis* infective stages (author's transl)]. Z. Parasitenkd. **54**, 101 – 124.

Qin, C.-L., Tang, J., Kim, K. (1998): Cloning and in vitro expression of TPK3, a *Toxoplasma gondii* homologue of shaggy/glycogen synthase kinase-3 kinases. Mol. Biochem. Parasitol. **93**, 273 – 282.

Satir, B., Schooley, C., Satir, P. (1972): Membrane reorganization during secretion in *Tetrahymena*. Nature **235**, 53 – 54.

Satir, B., Schooley, C., Satir, P. (1973): Membrane fusion in a model system. Mucocyst secretion in *Tetrahymena*. J. Cell Biol. **56**, 153 – 176.

Satir, B. H. (1989): Signal transduction events associated with exocytosis in ciliates. J. Protozool. **36**, 382 – 389.

Satir, B. H., Srisomsap, C., Reichman, M., Marchase, R. B. (1990): Parafusin, an exocytic-sensitive phosphoprotein, is the primary acceptor for the glucosylphosphotransferase in *Paramecium tetraurelia* and rat liver. J. Cell Biol. **111**, 901 – 907.

Sogin, M. L., Silberman, J. D. (1998): Evolution of the protists and protistan parasites from the perspective of molecular systematics. Int. J. Parasitol. **28**, 11 – 20.

Stelly, N., Halpern, S., Nicolas, G., Fragu, P., Adoutte, A. (1995): Direct visualization of a vast cortical calcium compartment in *Paramecium*

by secondary ion mass spectrometry (SIMS) microscopy: possible involvement in exocytosis. J. Cell Sci. **108**, 1895 – 1909.

Stelly, N., Mauger, J. P., Claret, M., Adoutte, A. (1991): Cortical alveoli of *Paramecium*: a vast submembranous calcium storage compartment. J. Cell Biol. **113**, 103 – 112.

Subramanian, S. V., Satir, B. H. (1992): Carbohydrate cycling in signal transduction: parafusin, a phosphoglycoprotein and possible $Ca^{(2+)}$-dependent transducer molecule in exocytosis in *Paramecium*. Proc. Natl. Acad. Sci. USA **89**, 11297 – 11301.

Subramanian, S. V., Wyroba, E., Andersen, A. P., Satir, B. H. (1994): Cloning and sequencing of parafusin, a calcium-dependent exocytosis-related phosphoglycoprotein. Proc. Natl. Acad. Sci. USA **91**, 9832 – 9836.

Zhao, H., Satir, B. H. (1998): Parafusin is a membrane and vesicle associated protein that cycles at exocytosis. Eur. J. Cell Biol. **75**, 46 – 53.

Zieseniss, E., Plattner, H. (1985): Synchronous exocytosis in *Paramecium* cells involves very rapid (less than or equal to 1 s), reversible dephosphorylation of a 65-kD phosphoprotein in exocytosis-competent strains. J. Cell Biol. **101**, 2028 – 2035.